Published in final edited form as:
Brain Res. 2013 July 3; 1520: 80–94. doi:10.1016/j.brainres.2013.04.032.

AMPA and $GABA_{A/B}$ Receptor Subunit Expression in the Cortex of Adult Squirrel Monkeys during Peripheral Nerve Regeneration

Todd M. Mowery[1], **Sarah M. Walls**[1], and **Preston E. Garraghty**[1,2]

[1]Department of Psychological and Brain Sciences, Indiana University Bloomington, IN

[2]Program in Neuroscience, Indiana University Bloomington, IN

Abstract

The primate somatosensory neuroaxis provides a highly translational model system with which to investigate adult neural plasticity. Here, we report immunohistochemical staining data for AMPA and $GABA_{A/B}$ receptor subunits in the area 3b cortex of adult squirrel monkeys one and five months after median nerve compression. This method of nerve injury was selected because it allows unique insight into how receptor expression changes during the regeneration of the peripheral nerve. One month after nerve compression, the pattern of subunit staining provides evidence that the cortex enters a state of reorganization. GABA 1 receptor subunits are significantly down-regulated in layer IV, V, and VI. Glur2/3 AMPA receptor subunits and postsynaptic $GABA_BR1b$ receptor subunits are up and down regulated respectively across all layers of cortex. After five months of recovery from nerve compression, the pattern of AMPA and $GABA_{A/B}$ receptor subunits remain significantly altered in a layer specific manner. In layer II/III, GluR1, GluR2/3, and GABA 1 subunit expression is significantly up-regulated while post synaptic $GABA_BR1b$ receptor subunits are significantly down regulated. In layer VI, V, and VI the GluR2/3 and presynaptic $GABA_BR1a$ receptor subunits are significantly up-regulated, while the postsynaptic $GABA_BR1b$ receptor subunits remain significantly down-regulated. Taken together, these results suggest that following nerve injury the cortex enters a state of reorganization that has persistent effects on cortical plasticity even after partial or total reinnervation of the peripheral nerve.

Introduction

The receptive field representations of adult neocortex are relatively stable due to a balance between excitatory and inhibitory processes that limit network sensitivity to changes in the pattern of peripheral inputs (for review, see Feldman 2009). While manipulations of peripheral inputs have been known to alter developmental processes since the early 1960's (e.g., Wiesel and Hubel 1963), demonstrations of the effects of deprivation on the mature brain emerged substantially later (Merzenich et. al. 1983a/b). Using a peripheral nerve injury

Address for Correspondence: Todd M. Mowery 4 Washington Place, NY, NY 10003 tm106@nyu.edu 812-929-1258.

model of sensory deprivation in non-human primates (median nerve transection), two phases of somatosensory plasticity were identified, one immediate, and the other more protracted. The immediate, “unmasking” phase of the cortical response to the loss of sensory inputs, evident minutes to hours after nerve transection, was characterized by an expansion in the representations of skin surfaces on the hand with intact innervation. However, most of the deprived cortex could not be activated by cutaneous peripheral stimulation at this time. Over the ensuing days to weeks after injury, the remaining deprived cortex came to express new receptive fields conveyed by the intact nerves to the hand.

In a subsequent paper, Wall et al. (1983) examined the process of recovery from peripheral nerve injury in a nerve compression model. This approach permitted the introduction of sensory loss that was identical to that accomplished with nerve transection (Merzenich et al., 1983a/b), but with nerve compression, the injured median nerve regenerated and reinnervated skin surfaces that had been deafferented by the manipulation. Electrophysiological mapping of the cortex at various time points after the nerve compression revealed that reorganization of median nerve cortex proceeded during the period in which the nerve was regenerating. Subsequently, as the regenerating median nerve reinnervated the hand, reactivation of the median nerve cortex by medial nerve territory on the hand proceeded sequentially from proximal (i.e., palm) to distal (i.e., digit tips) skin sites. Following complete regeneration, the map of the median nerve territory in cortex was indistinguishable from the one that existed prior to nerve injury (Wall et al. 1983).

Over the last two decades, our laboratory has used the mature non-human primate somatosensory system to systematically investigate the contributions of glutamatergic and GABAergic mechanisms to the process of reorganization that follows deprivation (Garraghty et al. 1991, 2006; Garraghty and Muja 1996; Myers et. al. 2000; Wellman et. al. 2002; Mowery and Garraghty 2009; Mowery et. al. 2011; Sarin, Mowery, and Garraghty 2012). Our studies have provided evidence that AMPA and GABA receptors play key roles in the adult brain's response to sensory deprivation. In our most recent studies we have used the median nerve compression model of sensory deprivation to undertake a series of immunohistochemical studies designed to focus on the changes to AMPA and GABA receptor subunit expression following deprivation, reorganization, and, ultimately reinnervation. Nerve compression (or crush) is uniquely different from other forms of nerve injury in that the peripheral nerve regenerates along an intact neural sheath; essentially reinnervating original cutaneous skin receptors (Barbay et al., 2002, Kis et al., 1999 and Wall et al., 1983). Re-establishment of original topography is more complete than what has been reported for other nerve regeneration paradigms (e.g. transection and repair — Wall and Kaas, 1986).

Using this technique we previously reported that there are significant changes in AMPA and $GABA_{A/B}$ receptor subunits one week after median nerve compression, and that the resulting patterns of subunit immunostaining closely resemble ones found early in development (Mowery and Garraghty 2009; Mowery et. al. 2011; Sarin, Mowery, and Garraghty 2012). The current studies extend those observations to one month and five months after median nerve compression. At one month after the nerve injury, the cortex shows evidence of having undergone reorganization. Five months after median nerve

compression, a time when any ongoing nerve regeneration should be complete, the pattern of AMPA and GABA receptors suggests that the affected region of cortex has regained primary inhibitory tone ($GABA_A$) and yet retains increased potential for NMDA mediated plasticity.

Methods

Nerve Compression

We report data from 5 adult squirrel monkeys (*Saimiri sciureus*) that underwent median nerve compressions. Animals survived for either 1 month (N=2) or 5 months (N=3). Animals were maintained on isoflurane anesthesia (2–4%) throughout the surgery. The ventral forearm was shaved between the wrist and elbow, and an incision was made along its midline 70 mm from the wrist. Under microscopic view, the median nerve was located and isolated by blunt dissection and then elevated. The nerve was compressed with hemostats at a 45° angle and held in place for 30 seconds. Compression was repeated three times distally over the span of a few mm to ensure complete axonal compression. The hemostat was rotated 90°, and the process was repeated 3 more times to create a crossing pattern (adapted from Wall et al., 1983). The nerve was repositioned, the skin was sutured over the incision site, and the animal was allowed to recover. All protocols were approved by the Institutional Animal Care and Use Committee (IACUC).

Immunohistochemistry

After one month or five months of recovery, animals were anesthetized with isoflurane gas and transcardially perfused with cold 0.9% saline solution followed by 400 ml of 4% paraformaldehyde in 0.1 M phosphate buffer (pH 7.4). Following perfusion the brain was extracted and the left and right somatosensory cortices were dissected out and post-fixed for 2 h in cold fixative (4% paraformaldehyde in 0.1 M phosphate buffer (pH 7.4). Tissue was cryoprotected overnight in 30% sucrose in phosphate buffer (pH 7.4).

Sectioning

Frozen 40 m sections of the pre and post-central gyri were cut in a coronal plane and collected in staining nets in phosphate buffer. Sections that clearly contained tissue including the central sulcus were kept for immunohistochemistry. To decrease staining inconsistencies within animals, left and right hemispheres were stained simultaneously in 4 in^2 wells that contained 8 (1 × 2 in.) wells. These were placed 5 across and 5 down in staining vessels (20 1/2 in^2). During primary antibody staining, tissue was incubated in and washed in separate staining vessels (4 1/2 × 20 in.).

Staining

After sectioning, tissue was washed in immuno-phosphate buffer (IPB) and incubated in blocking solution for 30 min followed by hydrogen peroxide .01% for 15 min at room temperature to reduce endogenous peroxidase activity. Tissue sections were incubated overnight at 4 °C in antisera containing GluR1 (1:1000 Chemicon), GluR2/3 (1:1000 Thermo Scientific), $GABA_A$ 1 (1: 1000 Thermo Scientific), $GABA_B$1a (1:1000 Alpha Diagnostics International), or $GABA_B$1b (1:1000 Alpha Diagnostics International), and

washed three times for ten minutes in IPB before being incubated in goat anti-rabbit biotinylated antibodies for 1 h at room temperature. Sections were again washed three times for ten minutes in PBS, incubated in ABC solution for one hour (ABC Elite Kit, Vector), washed again three times for ten minutes in Acetate-Imidazole buffer, and incubated in Acetate-Imidazole buffer containing Nickel Sulfate, 0.5 mg/ml 3.3 -diaminobenzidine-4HCI (DAB, Vector) and 0.01% H2O2 for approximately 8 min. Sections were washed three times in PBS for ten minutes, mounted on gelatin coated glass slides and dried overnight. Once dry, the sections were dehydrated in ascending ethanols, cleared with xylenes, and cover-slipped. Positive and negative controls were generated by omitting the primary or secondary antibody. Light microscopy of tissue did not reveal the presence of any non-specific binding. Separate lots of antibodies were used between animals, but the quantified difference in the pattern of staining was the same in each animal for each subunit. See **Table 1** for a list of antibodies.

Luminance/Densitometry

Immunohistochemical quantification of tissue sections was carried out as previously described (Mowery and Garraghty, 2009) at 1480× under brightfield illumination using a microscope (Nikon Eclipse 80i; Nikon Instruments; Melville, NY, USA) and the Stereo Investigator software (MBF Bioscience; Williston, VT, USA). The Stereo Investigator software's luminance function (formerly densitometry/optical density) was used to quantify staining intensity of the traced contours (representative soma, neuropil, and white matter). The luminance function measures the amount of light passing through the tissue per μm^2 of contour (0 = black and 256 = white), and in this study was used as an indirect measurement of stained subunit protein expression (based on the principles of densitometry/ absorptiometry).

Great effort was made to maintain light parameters within the Stereo Investigator software between users and user sessions. Experimental and control data were collected on the same day under the same light parameters whenever possible. Video settings on the camera were saved once at the beginning of data collection and reloaded every user session. Each day at the beginning of data quantification, light settings were set to approximately 122 (gain) and 55.119 ms (exposure). The camera feed was set between “binocular” and “camera” settings. The condenser was set to the “up” position, and the diaphragm was fully open.

Tissue was focused at 4× and light settings were set to reflect a normal curve on the video histogram. The objective was switched to 40×, and the ND8 and ND32 filters were set to the “out” position. A normal light curve was re-established so that white matter was below the threshold of the histogram (256). After this, no adjustments were made to the settings throughout the duration of the session. When feasible, in an effort to limit variability, quantification was carried out per antibody within a single user session per animal. By switching the filters on and off, we were able to go between 4× and 40× without adjusting the light parameters, which reduced section to section variability even further.

Area 3b

Electrophysiological receptive field mapping was not used in this study as craniotomy and electrode penetration would introduce unknown and uncontrolled variables into the experimental design. The somatotopic representations referred to throughout this study are based on receptive field mapping observations we and others have consistently reported and are therefore approximations of the cortical regions corresponding to the injured nerves. The median nerve compression created a deprived state within a large region of area 3b cortical tissue corresponding to digits 1–3 (Garraghty et al., 2006, Sur et al., 1982 and Wall, Fellman, and Kaas 1983). Therefore and area 1.5 mm posterior and 1.5 mm anterior to the central sulcus was dissected out. Along the anterior/posterior axis this section of tissue was comprised primarily of area 3b as indicated by extensive electrophysiological mapping (see Fig. 9 Sur et. al. 1982). Along the mediolateral axis this section spanned the natural anatomical boundaries imposed by the longitudinal fissure (medial) and the lateral fissure (lateral).

In our previous studies the central dimple of the central sulcus provides a reliable landmark for locating the hand representation in area 3b (Churchill et al., 1998, Garraghty et al., 1994, Garraghty and Muja, 1995, Schroeder et al., 1995 and Schroeder et al., 1997). Median nerve inputs (the region of interest) have been consistently recorded 1 mm posterior and 1 mm anterior to the central sulcus in a cortical region surrounding the central dimple (e.g., Gingold et al., 1991, Myers et al., 2000; Sur et al., 1982). Tissue was mounted with the anterior face of the tissue section down. In this way, tissue was sliced posterior to anterior starting with presumed area 1 and ending in area 3a. As tissue was sliced in a coronal plane along the A/P axis, only sections that contained the central dimple of the central sulcus were kept for staining. Sections prior to the central dimple (~ area 1) were discarded and slicing stopped once the dimple was no longer seen (~ area 3a). Within these sections, areas approximate to digit representations one through three were identified according to the medial lateral axis where they are consistently represented (see Fig. 1 - Garraghty et. al. 2006). Sampling was carried out in the center of this region that we posit contains neurons dominantly driven by digit two median nerve input.

Bounding Box

A 1 mm wide tracing grid was aligned approximately within the area 3b median nerve representation (~ digit 2), which is ~ 1 mm lateral to the central sulcus dimple. There are no clear histological boundaries between digits, so it is conceivable that the tracing grid sometimes included regions that receive thalamocortical inputs from digit 1 or 3; however, these remain within the experimental input zone. Once the tracing grid was placed, the user moved throughout the predefined cortical layers (II–IV approximate) tracing the somata of user defined neurons within a centrally placed bounding box (100 mm^2). Layers were discernable to the trained observer based on differences in packing density (4×) and neural phenotype (40×). Quantification was carried out in the middle of each layer, as there are no abrupt laminar boundaries.

Data Collection

Tissue was originally sliced at 40 μm, but following staining procedures and cover-slipping had a final tissue thickness of around 25 to 30 μm. The microscope was focused down through the z-plane to a depth of around 15 μm where uniformly stained somas within the plane of focus were randomly selected and traced within the bounding box (~ 30 per section). Additionally, within each cortical layer, neuropil measurements were taken (~ 10 per section). These were operationally defined as regions of tissue in which z-axis scrolling from the top to the bottom of the tissue revealed no somata. Finally white matter measurements were collected (~ 5 per section), that consisted of regions in which antibody binding was absent. Three to five sections were measured per antibody per hemisphere per animal generating around 90 –150 soma measurements and 30–50 neuropil measurements per hemisphere per antibody. Staining intensity data were generated by quantifying the ratio of each traced soma or neuropil luminance value over the average staining intensity of the white matter luminance values in that section. This transformed each data point into a percent darker than white matter score — also referred to as subunit staining intensity. For each animal average staining intensity was calculated for experimental and control area 3b layers II/III, IV, and V,VI soma and neuropil. This generated a total of six experimental and six experimental data points per animal.

To control for any differences in staining imposed by variability due to perfusion quality, nerve injury, or immunohistochemical reagents, averaged scores for each animal's experimental hemisphere data were compared to the control hemisphere data using paired comparisons. Despite possible differences in staining intensity, the effects reported in this study were consistent across animals. That is, a reported significant change in staining intensity is one that was consistent across the animals used in this study (See qualitative scatter-plots).

Quantification

To determine whether there was a general effect of nerve injury on receptor subunit expression, paired comparisons were made between data collected from experimental and control hemispheres. Receptor density varies between cortical layers (Geyer et. al. 1998; Rakic et.al. 1998; Shaw et. al. 1991; Young et al.,1990), as well as, between soma and neuropil (Karube, Kubota, and Kawaguchi 2004; Vickers et. al. 1993; Wang et. al. 2004). Because of this, two types of paired comparisons were used. One comparison determined whether significant increases or decreases were present between the layers of experimental and control area 3b cortex. In these analyses soma and neuropil data were collapsed across layer. A second comparison was used to determine whether soma or neuropil staining intensity significantly increased or decreased across layers of experimental and control area 3b cortex. In these analyses layer specific data was collapses across location. Both types of analysis lead to larger SEMs because of the natural variance in staining intensity between layer and location. Furthermore, the low number of animals used in these experiments decreased the power of all statistical analyses. While some analyses yielded results that approached significance ($p < .1$), only p values $< .05$ were considered significant.

Results

AMPAR and GABAR SUBUNIT EXPRESSION (1 MONTH)

GluR1 Subunit Staining Intensity (1 Month)—The average **GluR1** staining intensities for cytoarchitectonic area 3b cortical layers were compared within animals (N=2) between experimental and control hemispheres one month after median nerve compression. **GluR1** staining intensity scores were quantified in somata and neuropil of layers II/III, IV, and V/VI from a region of cortex that receives input from the median nerve (**Figure 1A/B**). **Figure 1B** presents a micrograph illustrating the region in which data was acquired. Samples from an area approximating digit two of the hand representation were taken immediately 1mm lateral to the central dimple (CD) of the central sulcus and extending no more than 2 mm laterally (demarcated by the bounding box; also see Sur et al., 1982). These conventions were the same for all data collected within this study.

Qualitative examples of somatic staining are presented in **Figure 1C**. The compared values for both animals are presented in **Figure 1D**. These data show no obvious trends for either animal. **Figure 1E** shows that there were no differences between experimental and control hemispheres for data collected within **soma** [mean ± SEM; experimental 105.52 ± 16.67 vs. control 104.97 ± 17.28; t (5) = .72 p = .50]. There were also no differences in **neuropil** staining intensity [mean ± SEM; experimental 70.05 ± 15.22 vs. control 68.80 ± 15.33; t (5) = .78 p = .47]. As shown in **Figure 1F**, comparing staining intensity data across experimental and control cortical layers revealed no significant differences in layers **II/III** [mean ± SEM; experimental 132.29 ± 9.48 vs. control 132.33 ± 10.91; t (3) = .021, p = .98], **IV** [mean ± SEM; experimental 46.78 ± 6.22 vs. control 45.40 ± 6.21 t (3) = 1.21, p = .31], or **V/VI** [mean ± SEM; experimental 84.29 ± 15.36 vs. control 82.93 ± 15.37 – t (3) = 1.06 p = .36].

GluR2/3 Subunit Staining Intensity (1 Month)—The average **GluR2/3** staining intensities for cytoarchitectonic area 3b cortical layers were compared within the soma and neuropil of layers II/III, IV, and V/VI for the experimental and control hemispheres of animals (N = 2) one month after median nerve compression. **Figure 2A** presents qualitative examples of **GluR2/3** expression in control and experimental sections of II/III, IV, and V/VI layers of cortex. The compared data show a trend towards increased GluR2/3 staining intensity in both animals across layers and within soma and neuropil (**Figure 2B**). As seen in **Figure 2C**, statistical comparison revealed a significant increase in neuronal **soma** staining intensity between control and experimental hemispheres [mean ± SEM; experimental 91.65 ± 16.48 vs. control 83.61 ± 15.95 – t (5) = 3.09 p = .027]. This significant increase was also found within the **neuropil** [mean ± SEM; experimental 69.84 ± 13.00 vs. control 57.28 ± 13.03 – t (5) = 4.89, p = .004]. In **figure 2D,** paired comparison between the cortical layers of experimental and control hemispheres revealed a significant increase in layer **II/III** [mean ± SEM; experimental 122.32 ± 8.64 vs. control 112.66 ± 10.20 – t (3) = 3.65, p = .035], **IV** [mean ± SEM; experimental 41.99 ± 3.00 vs. control 35.95 ± 4.66 – t (3) = 3.43, p = .041], and **V/VI** subunit staining intensity [mean ± SEM; experimental 77.93 ± 7.60 vs. control 62.71 ± 9.89 – t (3) = 4.03, p = .027].

$GABA_A$ α 1 Subunit Staining Intensity (1 Month)—The average **$GABA_A$ 1** staining intensities for cytoarchitectonic area 3b cortical layers were compared within the soma and neuropil of layers II/III, IV, and V/VI for the experimental and control hemispheres of animals (N = 2) one month after median nerve compression. **Figure 3A** presents qualitative examples of **$GABA_A$ 1** expression in control and experimental sections of II/III, IV, and V/VI layers of cortex. The compared values from both animals show trends indicative of reduced staining intensity for neuropil and layer IV and V/VI in the experimental hemisphere, but no change in layer II/III soma staining intensity (**Figure 3B**). As seen in **figure 3C,** paired comparison revealed a non-significant effect of nerve-injury on **$GABA_A$ 1** subunit staining intensity within experimental soma (mean ± SEM; experimental 76.26 ± 16.63 vs. control 79.87 ± 14.61 – t (5) = 1.48 p = .197). Staining intensity within the neuropil; however, was significantly decreased [mean ± SEM; experimental 49.79 ± 12.54 vs. control 57.05 ± 11.12 – t (5) = 4.69, p = .005]. **Figure 3D** shows the paired comparisons for subunit staining intensity between experimental and control cortical layers. As the trends across both animals indicated, there was not a significant difference in staining intensity within layer II/III [mean ± SEM; experimental 106.51 ± 11.19 vs. control 106.50 ± 9.49 – t (3) = .004, p = .996]. There was a significant decrease in staining intensity for measurements taken in the experimental hemispheres of cortical layers **IV** [mean ± SEM; experimental 29.34 ± 4.11 vs. control 38.04 ± 3.42 – t (3) = 6.84, p = .006], and **V/VI** [mean ± SEM; experimental 53.23 ± 8.80 vs. control 60.84 ± 7.84 – t (3) = 3.58, p = .037].

$GABA_B$R1a Subunit Staining Intensity (1 Month)—The average **$GABA_B$R1a** staining intensities for cytoarchitectonic area 3b cortical layers were compared within the somata and neuropil of layers II/III, IV, and V/VI for the experimental and control hemispheres of animals (N = 2) one month after median nerve compression. **Figure 4A** presents qualitative examples of **$GABA_B$R1a** staining intensity in the soma of control and experimental sections of II/III, IV, and V/VI layers of cortex. The compared data for both animals in **Figure 4B** show no clear trends for changes in subunit staining intensity. Statistical comparison (**Figure 4C**) indicates that there were no differences in staining intensity for **soma** [mean ± SEM; experimental 68.07 ± 14.89 vs. control 69.40 ± 14.22 – t (5) = .418 p = .693] or **neuropil** measurements [mean ± SEM; experimental 46.65 ± 11.88 vs. control 46.13 ± 11.75 – t (5) = .418 p = .693]. Furthermore **Figure 4D** indicates that there were also no significant difference for subunit staining intensity within experimental cortical layers **II/III** [mean ± SEM; experimental 97.51 ± 9.05 vs. control 96.00 ± 9.41 – t (3) = .659 p = .556], **IV** [mean ± SEM; experimental 27.66 ± 3.88 vs. control 29.15 ± 4.70 – t (3) = 1.78, p = .17], or **V/VI** [mean ± SEM; experimental 48.15 ± 7.58 vs. control 46.91 ± 9.08 – t (3) = .678 p = .546].

$GABA_B$R1b Subunit Staining Intensity (1 Month)—The average **$GABA_B$R1b** staining intensities for cytoarchitectonic area 3b cortical layers were compared within the somata and neuropil of layers II/III, IV, and V/VI for the experimental and control hemispheres of animals (N = 2) one month after median nerve compression. **Figure 5A** presents qualitative examples of **$GABA_B$R1b** expression in control and experimental sections of II/III, IV, and V/VI layers of experimental and control cortex. Compared data for both animals shows a clear trend towards a decrease in subunit staining intensity across all

layers within soma and neuropil **(Figure 5B)**. Statistical comparison in **Figure 5C** shows significant decreases for staining intensity within the **soma** [mean ± SEM; experimental 78.47 ± 15.17 vs. control 92.72 ± 15.85 – t (5) = 2.76, p = .0398] and **neuropil** of neurons within the experimental hemisphere [mean ± SEM; experimental 51.78 ± 14.37 vs. control 64.11 ± 13.29 – t (5) = 3.35, p = .020]. **Figure 5D** shows that the significant decrease was also seen in experimental cortical layers **II/III** [mean ± SEM; experimental 106.70 ± 10.10 vs. control 119.70 ± 10.48 – t (3) = 3.21, p = .048], **IV** [mean ± SEM; experimental = 32.57 ± 6.33 vs. control 42.53 ± 5.58 – t (3) = 4.02, p = .027], and **V/VI** [mean ± SEM; experimental 56.11 ± 13.08 vs. control 73.00 ± 11.24 – t (3) = 3.78, p = .034].

AMPAR and GABAR Subunit Expression (5 Months)

GluR1 Subunit Staining Intensity (5 Months): The average **GluR1** staining intensities for cytoarchitectonic area 3b cortical layers were compared within the soma and neuropil of layers II/III, IV, and V/VI for the experimental and control hemispheres of animals (N = 3) five months after median nerve compression. **Figure 6A** presents qualitative examples of **GluR1** staining intensity in the soma of control and experimental sections of II/III, IV, and V/VI layers of cortex. The compared data from all three animals only show a trend of decreased staining intensity in layers II/III of experimental cortex (**Figure 6B**). Comparison of staining intensity data collected from the **soma** [mean ± SEM; experimental 83.42 ± 9.24 vs. control 83.67 ± 9.61 – t (8) = .493 p = .63] and **neuropil** [mean ± SEM; experimental 49.22 ± 6.45 vs. control 47.16 ± 7.19 – t (8) = 2.11 p = .067] of experimental and control hemispheres show no significant difference (**Figure 6C**). **Figure 6D** shows a significant decrease in receptor subunit expression in layer II/III [mean ± SEM; experimental 90.80 ± 8.21 vs. control 92.35 ± 8.25 – t (5) = 2.83, p = .036], but no changes for layers **IV** [mean ± SEM; experimental 38.39 ± 4.54 vs. control 36.29 ± 5.00 – t (5) = 3.39, p = .019], or **V/VI** [mean ± SEM; experimental 69.77 ± 10.68 vs. control 67.61 ± 11.72 – t (3) = 1.06 p = .36].

GluR2/3 Subunit Staining Intensity (5 Months): The average **GluR2/3** staining intensities for cytoarchitectonic area 3b cortical layers were compared within the soma and neuropil of layers II/III, IV, and V/VI for the experimental and control hemispheres of animals (N = 3) five months after median nerve compression. **Figure 7A** presents qualitative examples of **GluR2/3** expression in control and experimental cortical layers of II/III, IV, and V/VI. A trend towards increased staining intensity is seen for all three animals across experimental cortical layers, soma, and neuropil (**figure 7B**). Paired comparisons shown in **Figure 7C** indicate a significant nerve-injury induced increase in staining intensity for neuronal **soma** [mean ± SEM; experimental 62.61 ± 8.08 vs. control 59.82 ± 7.81 – t (8) = 4.05 p = .0037] and **neuropil** within the experimental hemisphere [mean ± SEM; experimental 41.10 ± 5.77 vs. control 38.63 ± 5.7 – t (8) = 4.08, p = .003]. As seen in **Figure 7D,** There was also a significant increase in staining intensity for layers **II/III** [mean ± SEM; experimental 73.31 ± 7.25 vs. control 70.05 ± 7.42 – t (5) = 2.92, p = .032], **IV** [mean ± SEM; experimental 29.07 ± 3.45 vs. control 27.19 ± 3.57 – t (5) = 7.19, p = .0008], and **V/VI** of the experimental hemisphere [mean ± SEM; experimental 53.18 ± 6.73 vs. control 50.18 ± 6.46 – t (5) = 3.77, p = .013].

$GABA_A$ α 1 Subunit Staining Intensity (5 Months): The average **$GABA_A$ 1** staining intensities for cytoarchitectonic area 3b cortical layers were compared within the somata and neuropil of layers II/III, IV, and V/VI for the experimental and control hemispheres of animals (N = 3) five months after median nerve compression. **Figure 8A** presents qualitative examples of **$GABA_A$ 1** expression in control and experimental cortical layers II/III, IV, and V/VI. The compared data show a trend towards a significant increase in receptor subunit staining intensity for layer II/III of the experimental hemisphere (**Figure 8B**). In **figure 8C**, paired comparison revealed no significant change in **$GABA_A$ 1** subunit staining intensity between experimental and control hemisphere **soma** [mean ± SEM; experimental 84.53 ± 9.73 vs. control 83.26 ± 9.63 – t (8) = 2.00 p = .080] and **neuropil** [mean ± SEM; experimental 52.63 ± 8.44 vs. control 51.92 ± 7.27 – t (8) = .499, p = .63]. **Figure 8D** shows that staining intensity data from experimental **II/III** layers did show a significant increase in staining intensity when compared to control data [mean ± SEM; experimental 99.30 ± 7.11 vs. control 95.60 ± 7.88 – t (8) = .3.98, p = .0105]. At the same time, staining intensity data for **IV** [mean ± SEM; experimental 37.86 ± 4.71 vs. control 38.45 ± 3.94 – t (8) = .656, p = .540], and **V/VI** cortical layers [mean ± SEM; experimental 68.57 ± 10.03 vs. control 68.72 ± 9.61 – t (8) = .108, p = .917] showed no significant difference.

$GABA_BR1a$ Subunit Staining Intensity (5 Months): The average **$GABA_BR1a$** staining intensities for cytoarchitectonic area 3b cortical layers were compared within the somata and neuropil of layers II/III, IV, and V/VI for the experimental and control hemispheres of animals (N = 3) five months after median nerve compression. **Figure 9A** presents qualitative examples of **$GABA_BR1a$** staining intensity in the soma of control and experimental cortical layers II/III, IV, and V/VI. **Figure 9B** shows that there was a trend towards increased subunit expression in layers IV, and V/VI of experimental hemispheres for all three animals. This trend was also seen for the soma and neuropil measurements across layers. Paired comparisons shown in **figure 9C** indicates a significant increase in **$GABA_BR1a$** subunit staining intensity for both neuronal **soma** [mean ± SEM; experimental 64.45 ± 7.76 vs. control 61.14 ± 8.21 – t (8) = 3.08 p = .015] and **neuropil** of experimental hemispheres [mean ± SEM; experimental 42.11 ± 5.33 vs. control 39.09 ± 5.85 – t (8) = 2.78 p = .023]. **Figure 9D** shows that this increase was not present in cortical layers **II/III** [mean ± SEM; experimental 74.05 ± 7.16 vs. control 73.36 ± 7.27 – t (5) = .659 p = .905]; however, there were significant increases in layers **IV** [mean ± SEM; experimental 31.40 ± 3.08 vs. control 28.25 ± 3.32 – t (5) = 2.64, p = .045] and **V/VI** of experimental hemispheres [mean ± SEM; experimental 54.39 ± 6.69 vs. control 48.73 ± 6.98 – t (5) = .5.35 p = .003].

$GABA_BR1b$ Subunit Staining Intensity (5 Months): The average **$GABA_BR1b$** staining intensities for cytoarchitectonic area 3b cortical layers were compared within the soma and neuropil of layers II/III, IV, and V/VI for the experimental and control hemispheres of animals (N = 3) five months after median nerve compression. **Figure 10A** presents qualitative examples of **$GABA_BR1b$** expression in control and experimental sections of II/III, IV, and V/VI layers of cortex. The compared data shows a clear trend in all three animals of decreases in subunit staining intensity across all layers for both soma and neuropil (**Figure 10B**). As seen in figure **Figure 10C,** paired comparisons revealed a significant nerve-injury induced decrease in **$GABA_BR1b$** subunit staining intensity between

experimental and control hemispheres for **soma** [mean ± SEM; experimental 63.61 ± 8.09 vs. control 79.24 ± 7.97 – t (8) = 4.57, p = .0018] and **neuropil** measurements [mean ± SEM; experimental 41.05 ± 6.51 vs. control 53.89 ± 7.97 – t (8) = 3.43, p = .008]. **Figure 10D** shows that there was also a significant decrease in experimental cortical layers **II/III** [mean ± SEM; experimental 76.29 ± 6.85 vs. control 97.09 ± 6.93 – t (5) = 5.53, p = .002], **IV** [mean ± SEM; experimental = 28.77 ± 3.92 vs. control 36.44 ± 3.90 – t (5) = 2.60, p = .047], and **V/VI** [mean ± SEM; experimental 51.60 ± 7.07 vs. control 66.30 ± 8.22 – t (5) = 3.28, p = .021].

Discussion

In this study we continue a series of experiments that investigated the immunostaining of AMPA and GABA receptor subunits in cytoarchitectonic area 3b of monkey cortex following median nerve compression. This injury model was selected because it offers the opportunity examine the changes in several targeted neurotransmitter subunits as the cortex undergoes the process of topographic reorganization and peripheral nerve reinnervation (Merzenich et al., 1983a, b; Wall et al., 1983; Schroeder et al., 1997; Wall et al., 1983). To that end, we find that the pattern of subunit expression provides insight into the receptor phenotypes that are altered during cortical reorganization (Garraghty et. al. 2006), and also suggests that changes in cortical receptor expression persist even following regenerating nerve injuries.

Unmasking & Developmental Recapitulation

The unmasking phase of somatosensory reorganization occurs immediately after the loss of peripheral inputs (Merzenich et. al. 1983b; Calford and Tweedale 1991; Myers et al. 2000). During this phase, masked latent inputs are disinhibited and immediately expressed as islands of novel somatotopic representations. The shift in receptor expression during the unmasking phase is characterized by a significant decline in $GABA_A$ receptors in the deprived cortex (Wellman et. al. 2002; Garraghty et. al. 2006). This neuronal response to pathophysiological conditions likely serves as an essential priming step for the induction of developmental-like plasticity in the adult system (Rivera et al., 1999, 2005).

A few days after nerve injury, GABAR withdrawal (Casasola et al., 2004 and Silva-Barrat et al., 1989) induces an intermediate state of plasticity characterized by a pattern of neuronal activity and receptor correlates that resemble a recapitulation of developing neocortex (physiology - Lenz et al., 1989, 1998; Dykes et al., 1995; Bergenheim et al., 2004; Sun et al., 2005; receptor expression - Mowery and Garraghty 2009; Mowery et. al. 2011; Sarin et al., 2012). For example, spontaneous neuronal activity takes on the bursting characteristics of developing neurons (Feller, 1999), and AMPA and $GABA_{A/B}$ subunits are up and down regulated into a pattern of expression described in developing systems (AMPA - Eybalin et al., 2004, Ho et al., 2007, Kumar et al., 2002; Whitney et al., 2008; GABA - Fritschy et al., 1999; McLean et al., 1996; Fukuda et al., 1993). This intermediate state has been suggested to be an important priming step for continued reorganization (Cusick et. al. 1990).

Reorganization and Onset of Reinnervation

The second stage of the cortical response to nerve injury involves the progressive reorganization of somatosensory receptive fields in the weeks following nerve injury (Merzenich et. al. 1983a; Schroeder et al., 1997). One month after median nerve transection, the cortex has undergone reorganization (Garraghty and Muja, 1996); however, with median nerve compression, the reinnervation of the hand by the regenerating median nerve is just beginning (see Figure 2; Wall et al. 1983). While the physiological state of the cortex was not investigated in this study, the pattern of results we report here is similar to those described for AMPA and $GABA_{A/B}$ receptors in experiments that use a non-regenerating form of nerve injury. For example, AMPA receptor numbers were elevated across all cortical layers one to two months after nerve transection (Garraghty et al., 2006). For the nerve transected monkeys, we argued that the increase in AMPA receptors paralleled reports of increases in AMPA receptor expression in the hippocampus found after NMDA receptor-dependent LTP (e.g., Tocco et al., 1992; Maren et al., 1993). Presumably, NMDA receptor-dependent plasticity mechanisms are operating in the deprived cortex after nerve compression as well. A significant elevation in the GluR1/2 containing AMPAR would presumably be accompanied by a significant increase in GluR1 receptor expression which we find no evidence of. Therefore, we would posit that the previously unrevealed AMPAR species would be those containing the GluR2/3 subunits. Which were significantly elevated across all layers and locations.

The pattern of expression for $GABA_A$ α1 subunit staining intensity is very similar to that found 1-2 months after median nerve transection (Garraghty et al., 2006; Fig. 2). In that study we reported a significant decrease in the number of $GABA_A$ receptors in layers VI and V/VI. In the current study $GABA_A$ α1 subunit expression is also significantly lowered in IV and V/VI layers while indicating no change in layers II/III. Given that the 1 subunit is predominantly found in the mature $GABA_A$ receptor phenotype (1 α1, 2 α2, and 2 y2 subunits – Golshani et al., 1997) we maintain that the result from the current study corroborates our previous finding.

In our previous study $GABA_B$ expression was significantly reduced in IV and V/VI layers during reorganization; however, the isoform of the $GABA_B$ receptor remained unknown (Garraghty et. al. 2006). The presynaptic $GABA_BR1a$ subunit staining intensity is not significantly different from controls at this time suggesting this receptor isoform did not contribute to the significant decrease in $GABA_B$ receptor expression. Instead our results suggest that the $GABA_BR1b$ containing postsynaptic isoform (Benke et. al. 1999) is significantly down-regulated after nerve injury. A parsimonious explanation for this highly significant decrease in subunit density is that prolonged activation of NMDA receptors induces a large scale endocytocis of the postsynaptic $GABA_B$ receptor (Terunuma et. al. 2010). Furthermore, the postsynaptic $GABA_B$ receptor has been shown to inhibit the function of NMDA receptors (e.g., Otmakhova and Lisman, 2004). Thus, a significant reduction in postsynaptic $GABA_B$ would in turn serve to facilitate the ongoing process of NMDA dependent reorganization (Garraghty and Muja 1996).

Reinnervation and Recovery

In this study we used a form of nerve compression injury that has been reported to induce peripheral reinnervation of the hand and distal digit tips ~ 3 months after nerve compression (Wall et al., 1983). That is, the centrally-projecting afferents once again activated neurons topographically across the appropriate sector of cortical area 3b. For this study a survival duration of five months was selected to promote full regeneration of the median nerve; however, it is important to note that the complete recovery from peripheral nerve injury in humans and animal models has been reported to vary on an individual basis (eg Gordon et. al. 2007; Ronchi et. al 2009). No electrophysiological data was acquired from these animals and the state of functional reactivation of cortex is unknown. Therefore the results from this study should be interpreted as coming from a region of cortex that has undergone acute deprivation and reorganization with possible reactivation by original peripheral receptors following partial or full reinnervation of the compressed nerve.

Regardless, the pattern of subunit expression is different from that reported at 1 month post injury; suggesting a different state of plasticity. Furthermore it varies between layers II/III, and layers VI, V, and VI. Specifically the upper layers have significantly elevated levels of GluR1 and GluR2/3. This could suggest that both the GluR1/2 and GluR2/3 receptor isoforms of AMPA receptor have been up-regulated, providing evidence of increased NMDA dependent LTP within this system (Tocco et al., 1992; Maren et al., 1993). At the same time, we report a significant increase in $GABA_A$ α1 subunit, and this could indicate a concomitant increase in $GABA_A$ receptor subunits. Finally the presynaptic $GABA_B$ receptor is not significantly different from controls while the postsynaptic $GABA_B$ receptor is significantly decreased. From a plasticity perspective this pattern suggests that inhibitory mechanisms have been up-regulated in layer II/III to balance the heightened excitatory tone inherent to an increase in AMPA receptors and a decrease in the NMDAR inhibiting post synaptic $GABA_B$ receptor (Otmakhova and Lisman 2004).

The second pattern of subunit expression is seen in layer IV, V, and VI. In these layers, GluR1 is not significantly different from controls, while GluR2/3 remains significantly elevated. Like the results reported at 1 month, this suggests that the GluR2/3 containing AMPARs remain up-regulated. Unlike layer II/III, $GABA_A$ α1 is not significantly different from controls while auto-regulatory presynaptic $GABA_BR$ is significantly up-regulated. This suggests decreased GABA neurotransmitter release and subsequently lower inhibitory tone. At the same time the postsynaptic GABABR is significantly decreased, again suggesting disinhibition of the NMDAR (Otmakhova and Lisman 2004). This is not surprising considering that prolonged NMDAR activation promotes a significant endocytosis of these receptors (Terunuma et. al. 2010) and reorganization is an NMDA dependent process (Myers et. al. 2000). Taken together this pattern of subunit expression suggests that these layers are more plastic. That is, a decrease in inhibitory tone, specifically for NMDAR, and an increase in the excitatory mediating GluR2/3 AMPAR suggest that there is an increased probability of long-term potentiation within these neural networks (Davies et al., 1991; Davies and Collingridge, 1996; Mott and Lewis 1992; Stäubli, Scafidi, and Chun 1999).

Conclusion

In many sensory systems, traces of transient reorganization persist long after recovery (Froemke, Merzenich, and Schreiner 2007; Woolf et. al. 1995). At the same time, original somatotopic representations are retained in the reorganized cortex of humans with long standing nerve injuries (Shady 1994; Moore and Schady 2000 Halligan et. al. 1993). These original somatotopic representations are perceived during electrical activation of nerve stumps suggesting that the cortex retains traces of past plasticity. Here we provide evidence that the primary somatosensory cortex has layer specific patterns of plasticity related receptor expression after a regenerating nerve injury. It is possible that these persistent up and down regulations of receptor subunits facilitate or represent the preservation of neuroanatomical changes that occur during reorganization.

Acknowledgments

Supported by National Institutes of Health/National Institute of Neurological Disorders and Stroke; Grant number: NS37348.

Literature Cited

Alitto HJ, Usrey WM. Corticothalamic feedback and sensory processing. Curr Opin Neurobiol. 2003; 13:440–5. [PubMed: 12965291]

Allard T, Clark SA, Jenkins WM, Merzenich MM. Reorganization of somatosensory area 3b representations in adult owl monkeys after digital syndactyly. J Neurophysiol. 1991; 66:1048–1058. [PubMed: 1753275]

Alloway KD, Burton H. Differential effects of GABA and bicuculline on rapidly- and slowly-adapting neurons in primary somatosensory cortex of primates. Exp Brain Res. 1991; 85:598–610. [PubMed: 1655509]

Bartley AF, Huang ZJ, Huber KM, Gibson JR. Differential activity-dependent, homeostatic plasticity of two neocortical inhibitory circuits. J Neurophysiol. 2008; 100:1983–94. [PubMed: 18701752]

Canedo A, Mariño J, Aguilar J. Lemniscal recurrent and transcortical influences on cuneate neurons. Neuroscience. 2000; 97:317–34. [PubMed: 10799764]

Casasola C, Montiel T, Calixto E, Brailowsky S. Hyperexcitability induced by GABA withdrawal facilitates hippocampal long-term potentiation. Neuroscience. 2004; 126:163–71. [PubMed: 15145082]

Churchill JD, Arnold LL, Garraghty PE. Somatotopic reorganization in the brainstem and thalamus following peripheral nerve injury in adult primates. Brain Res. 2001; 910:142–152. [PubMed: 11489264]

Churchill JD, Muja N, Myers WA, Besheer J, Garraghty PE. Somatotopic consolidation: a third phase of reorganization after peripheral nerve injury in adult squirrel monkeys. Exp Brain Res. 1998; 118:189–196. [PubMed: 9547087]

Churchill JD, Tharp JA, Wellman CL, Sengelaub DR, Garraghty PE. Morphological correlates of injury-induced reorganization in primate somatosensory cortex. BMC Neurosci. 2004; 5:43. [PubMed: 15533258]

Collingridge GL, Randall AD, Davies CH, Alford S. The synaptic activation of NMDA receptors and Ca^{2+} signalling in neurons. Ciba Found Symp. 1992; 164:162–71. [PubMed: 1327677]

Coq JO, Barr AE, Strata F, Russier M, Kietrys DM, Merzenich MM, Byl NN, Barbe MF. Peripheral and central changes combine to induce motor behavioral deficits in a moderate repetition task. Exp Neurol. Dec; 2009 220(2):234–45. 2009. [PubMed: 19686738]

Courtine G, Bunge MB, Fawcett JW, Grossman RG, Kaas JH, Lemon R, Maier I, Martin J, Nudo RJ, Ramon-Cueto A, Rouiller EM, Schnell L, Wannier T, Schwab ME, Edgerton VR. Can

experiments in nonhuman primates expedite the translation of treatments for spinal cord injury in humans? Nat Med. 2007; 13:561–6. [PubMed: 17479102]

Cramer SC, Chopp M. Recovery recapitulates ontogeny. Trends Neurosci. 2000; 23:265–271. [PubMed: 10838596]

Cramer SC, Riley JD. Neuroplasticity and brain repair after stroke. Curr Opin Neurol. 2008; 21:76–82. [PubMed: 18180655]

Dableh L, Yashpal K, Henry J. Neuropathic pain as a process: reversal of chronification in an animal model. J Pain Res. 2011; 4:315–323. [PubMed: 22003305]

Dreher B, Burke W, Calford MB. Cortical plasticity revealed by circumscribed retinal lesions or artificial scotomas. Prog Brain Res. 2001; 134:217–46. [PubMed: 11702546]

Duffau H. Does post-lesional subcortical plasticity exist in the human brain? Neurosci Res. 2009; 65:131–5. [PubMed: 19616045]

Dunning DD, Hoover CL, Soltesz I, Smith MA, O'Dowd DK. GABA(A) receptor-mediated miniature postsynaptic currents and alpha-subunit expression in developing cortical neurons. J Neurophysiol. 1999; 82:3286–97. [PubMed: 10601460]

Ergenzinger ER, Glasier MM, Hahm JO, Pons TP. Cortically induced thalamic plasticity in the primate somatosensory system. Nat Neurosci. 1998; 1:226–229. [PubMed: 10195147]

Eybalin M, Caicedo A, Renard N, Ruel J, Puel JL. Transient Ca2+-permeable AMPA receptors in postnatal rat primary auditory neurons. Eur J Neurosci. 2004; 20:2981–2989. [PubMed: 15579152]

Faggin BM, Nguyen KT, Nicolelis MA. Immediate and simultaneous sensory reorganization at cortical and subcortical levels of the somatosensory system. Proc Natl Acad Sci USA. 1997; 94:9428–9433. [PubMed: 9256499]

Fagiolini M, Hensch TK. Inhibitory threshold for critical-period activation in primary visual cortex. Nature. Mar 9; 2000 404(6774):183–6. 2000. [PubMed: 10724170]

Feller MB. Spontaneous correlated activity in developing neural circuits. Neuron. 1999; 22:653–656. [PubMed: 10230785]

Florence SL, Wall JT, Kaas JH. Somatotopic organization of inputs from the hand to the spinal gray and cuneate nucleus of monkeys with observations on the cuneate nucleus of humans. J Comp Neurol. 1989; 286:48–70. [PubMed: 2475533]

Florence SL, Wall JT, Kaas JH. Central projections from the skin of the hand in squirrel monkeys. J Comp Neurol. 1991; 311:563–578. [PubMed: 1721925]

Fritschy JM, Meskenaite V, Weinmann O, Honer M, Benke D, Mohler H. GABAB-receptor splice variants GB1a and GB1b in rat brain: developmental regulation, cellular distribution and extrasynaptic localization. Eur J Neurosci. 1999; 11:761–8. [PubMed: 10103070]

Froemke RC, Merzenich MM, Schreiner CE. A synaptic memory trace for cortical receptive field plasticity. Nature. 2007; 450:425–9. 2007. [PubMed: 18004384]

Fukuda A, Mody I, Prince DA. Differential ontogenesis of presynaptic and postsynaptic GABAB inhibition in rat somatosensory cortex. J Neurophysiol. 1993; 70:448–452. [PubMed: 8395587]

Gaïarsa JL. Plasticity of GABAergic synapses in the neonatal rat hippocampus. J Cell Mol Med. 2004; 8:31–37. [PubMed: 15090258]

Garraghty PE, Arnold LL, Wellman CL, Mowery TM. Receptor autoradiographic correlates of deafferentation-induced reorganization in adult primate somatosensory cortex. J Comp Neurol. 2006; 497:636–645. [PubMed: 16739196]

Garraghty PE, Hanes DP, Florence SL, Kaas JH. Pattern of peripheral deafferentation predicts reorganizational limits in adult primate somatosensory cortex. Somatosens Mot Res. 1994; 11:109–117. [PubMed: 7976005]

Garraghty PE, Kaas JH. Functional reorganization in adult monkey thalamus after peripheral nerve injury. NeuroReports. 1991; 2:747–750.

Garraghty PE, LaChica EA, Kaas JH. Injury-induced reorganization of somatosensory cortex is accompanied by reductions in GABA staining. Somatosens Mot Res. 1991; 8:347–354. [PubMed: 1667058]

Garraghty PE, Muja N. Possible use-dependent changes in adult primate somatosensory cortex. Brain Res. 1995; 686:119–21. [PubMed: 7583265]

Garraghty PE, Muja N. NMDA receptors and plasticity in adult primate somatosensory cortex. J Comp Neurol. 1996; 367:319–326. [PubMed: 8708013]

Garraghty PE, Pons TP, Sur M, Kaas JH. The arbors of axons terminating in middle cortical layers of somatosensory area 3b in owl monkeys. Somatosensory and Motor Research. 1989; 6:401–411. [PubMed: 2756803]

Garraghty PE, Sur M. Morphology of single intracellularly stained axons terminating in area 3b of macaque monkeys. J Comp Neurol. 1990; 294:583–593. [PubMed: 2341626]

Geyer S, Matelli M, Luppino G, Schleicher A, Jansen Y, Palomero-Gallagher N, Zilles K. Receptor autoradiographic mapping of the mesial motor and premotor cortex of the macaque monkey. J Comp Neurol. 1998; 397:231–250. [PubMed: 9658286]

Ghosh A, Ginty DD, Bading H, Greenberg ME. Calcium regulation of gene expression in neuronal cells. J Neurobiol. 1994; 25:294–303. [PubMed: 7910846]

Golshani P, Truong H, Jones EG. Developmental expression of GABA(A) receptor subunit and GAD genes in mouse somatosensory barrel cortex. J Comp Neurol. 1997; 383:199–219. [PubMed: 9182849]

Guadagno JV, Warburton EA, Jones PS, Day DJ, Aigbirhio FI, Fryer TD, Harding S, Price CJ, Green HA, Barret O, Gillard JH, Baron JC. How affected is oxygen metabolism in DWI lesions?: a combined acute stroke PET-MR study. Neurology. 2006; 67:824–829. [PubMed: 16966545]

Gingold SI, Greenspan JD, Apkarian AV. Anatomic evidence of nociceptive inputs to primary somatosensory cortex: relationship between spinothalamic terminals and thalamocortical cells in squirrel monkeys. J Comp Neurol. 1991; 308:467–90. [PubMed: 1865012]

Gordon T, Brushart TM, Amirjani N, Chan KM. The potential of electrical stimulation to promote functional recovery after peripheral nerve injury--comparisons between rats and humans. Acta Neurochir Suppl. 2007; 100:3–11. 2007. [PubMed: 17985535]

Graziano A, Jones EG. Early withdrawal of axons from higher centers in response to peripheral somatosensory denervation. J Neurosci. 2009; 29:3738–48. [PubMed: 19321770]

Hagemann G, Redecker C, Neumann-Haefelin T, Freund HJ, Witte OW. Increased long-term potentiation in the surround of experimentally induced focal cortical infarction. Ann Neurol. 1998; 44:255–258. [PubMed: 9708549]

Halligan PW, Marshall JC, Wade DT, Davey J, Morrison D. Thumb in cheek? Sensory reorganization and perceptual plasticity after limb amputation. Neuroreport. 1993; 4:233–6. [PubMed: 8477042]

Hashimoto T, Nguyen QL, Rotaru D, Keenan T, Arion D, Beneyto M, Gonzalez-Burgos G, Lewis DA. Protracted developmental trajectories of GABAA receptor alpha1 and alpha2 subunit expression in primate prefrontal cortex. Biol Psychiatry. 2009; 65:1015–1023. [PubMed: 19249749]

Hayes C, Molloy AR. Neuropathic pain in the perioperative period. Int Anesthesiol Clin. 1997; 35:67–81. [PubMed: 9246582]

Hensch TK. Critical period mechanisms in developing visual cortex. Curr Top Dev Biol. 2005; 69:215–37. [PubMed: 16243601]

Henschel O, Gipson KE, Bordey A. GABAA receptors, anesthetics and anticonvulsants in brain development. CNS Neurol Disord Drug Targets. 2008; 7:211–24. [PubMed: 18537647]

Hicks TP, Dykes RW. Receptive field size for certain neurons in primary somatosensory cortex is determined by GABA-mediated intracortical inhibition. Brain Res. 1983; 274:160–4. [PubMed: 6137268]

Ho MT. Developmental expression of Ca2+-permeable AMPA receptors underlies depolarization-induced long-term depression at mossy fiber CA3 pyramid synapses. J Neurosci. 2007; 27:11651–11662. [PubMed: 17959808]

Huang ZJ. GABAB receptor isoforms caught in action at the scene. Neuron. 2006; 50:521–524. [PubMed: 16701201]

Hubner CA, Stein V, Hermans-Borgmeyer I, Meyer T, Ballanyi K, Jentsch TJ. Disruption of KCC2 reveals an essential role of K-Cl cotransport already in early synaptic inhibition. Neuron. 2001; 30:515–524. [PubMed: 11395011]

Irvine DR, Rajan R. Injury- and use-related plasticity in the primary sensory cortex of adult mammals: possible relationship to perceptual learning. Clin Exp Pharmacol Physiol. 1996; 23:939–947. [PubMed: 8911738]

Jain N, Florence SL, Qi HX, Kaas JH. Growth of new brainstem connections in adult monkeys with massive sensory loss. Proc Natl Acad Sci USA. 2000; 97:5546–5550. [PubMed: 10779564]

Jones KA, Borowsky B, Tamm JA, Craig DA, Durkin MM, Dai M, Yao WJ, Johnson M, Gunwaldsen C, Huang LY, Tang C, Shen Q, Salon JA, Morse K, Laz T, Smith KE, Nagarathnam D, Noble SA, Branchek TA, Gerald C. GABA(B) receptors function as a heteromeric assembly of the subunits GABA(B)R1 and GABA(B)R2. Nature. 1998; 396:674–679. [PubMed: 9872315]

Jones EG. Cortical and subcortical contributions to activity-dependent plasticity in primate somatosensory cortex. Annu Rev Neurosci. 2000; 23:1–37. 2000. [PubMed: 10845057]

Jones EG, Woods TM, Manger PR. Adaptive responses of monkey somatosensory cortex to peripheral and central deafferentation. Neuroscience. 2002; 111:775–97. [PubMed: 12031404]

Kaas JH, Qi HX, Burish MJ, Gharbawie OA, Onifer SM, Massey JM. Cortical and subcortical plasticity in the brains of humans, primates, and rats after damage to sensory afferents in the dorsal columns of the spinal cord. Exp Neurol. 2008; 209:407–416. [PubMed: 17692844]

Karube F, Kubota Y, Kawaguchi Y. Axon branching and synaptic bouton phenotypes in GABAergic nonpyramidal cell subtypes. J Neurosci. 2004; 24:2853–2865. [PubMed: 15044524]

Kaupmann K, Huggel K, Heid J, Flor PJ, Bischoff S, Mickel SJ, McMaster G, Angst C, Bittiger H, Froestl W, Bettler B. Expression cloning of GABA(B) receptors uncovers similarity to metabotropic glutamate receptors. Nature. 1997; 386:239–246. [PubMed: 9069281]

Kaupmann K, Malitschek B, Schuler V, Heid J, Froestl W, Beck P, Mosbacher J, Bischoff S, Kulik A, Shigemoto R, Karschin A, Bettler B. GABA(B)-receptor subtypes assemble into functional heteromeric complexes. Nature. 1998; 396:683–687. [PubMed: 9872317]

Kaupmann K, Schuler V, Mosbacher J, Bischoff S, Bittiger H, Heid J, Froestl W, Leonhard S, Pfaff T, Karschin A, Bettler B. Human gamma-aminobutyric acid type B receptors are differentially expressed and regulate inwardly rectifying K+ channels. Proc Natl Acad Sci USA. 1998; 95:14991–14996. [PubMed: 9844003]

Krupa DJ, Ghazanfar AA, Nicolelis MA. Immediate thalamic sensory plasticity depends on corticothalamic feedback. Proc Natl Acad Sci USA. 1999; 96:8200–8205. [PubMed: 10393972]

Kumar SS, Bacci A, Kharazia V, Huguenard JR. A developmental switch of AMPA receptor subunits in neocortical pyramidal neurons. J Neurosci. 2002; 22:3005–3015. [PubMed: 11943803]

Kuner R, Köhr G, Grünewald S, Eisenhardt G, Bach A, Kornau HC. Role of heteromer formation in GABAB receptor function. Science. 1999; 283:74–77. [PubMed: 9872744]

Laurie DJ, Wisden W, Seeburg PH. The distribution of thirteen GABAA receptor subunit mRNAs in the rat brain. III. Embryonic and postnatal development. J Neurosci. 1992; 12:4151–4172. [PubMed: 1331359]

Lenz FA, Kwan HC, Dostrovsky JO, Tasker RR. Characteristics of the bursting pattern of action potentials that occurs in the thalamus of patients with central pain. Brain Res. 1989; 496:357–60. [PubMed: 2804648]

Lenz FA, Garonzik IM, Zirh TA, Dougherty PM. Neuronal activity in the region of the thalamic principal sensory nucleus (ventralis caudalis) in patients with pain following amputations. Neuroscience. 1998; 86:1065–81. [PubMed: 9697114]

Liang F, Hatanaka Y, Saito H, Yamamori T, Hashikawa T. Differential expression of gamma-aminobutyric acid type B receptor-1a and -1b mRNA variants in GABA and non-GABAergic neurons of the rat brain. J Comp Neurol. 2000; 416:475–495. [PubMed: 10660879]

Liu Q, Wong-Riley MT. Developmental changes in the expression of GABAA receptor subunits alpha1, alpha2, and alpha3 in brain stem nuclei of rats. Brain Res. 2006; 1098:129–138. [PubMed: 16750519]

Lue JH, Jiang-Shieh YF, Shieh JY, Ling EA, Wen CY. Multiple inputs of GABA-immunoreactive neurons in the cuneate nucleus of the rat. Neurosci Res. 1997; 27(2):123–32. [PubMed: 9100254]

Lu XY, Ghasemzadeh MB, Kalivas PW. Regional distribution and cellular localization of gamma-aminobutyric acid subtype 1 receptor mRNA in the rat brain. J Comp Neurol. 1999; 407:166–182. [PubMed: 10213089]

Marik SA, Yamahachi H, McManus JN, Szabo G, Gilbert CD. Axonal dynamics of excitatory and inhibitory neurons in somatosensory cortex. PLoS Biol. 2010; 8:e1000395. [PubMed: 20563307]

McLean HA, Caillard O, Khazipov R, Ben-Ari Y, Gaiarsa JL. Spontaneous release of GABA activates GABAB receptors and controls network activity in the neonatal rat hippocampus. J Neurophysiol. 1996; 76:1036–1046. [PubMed: 8871218]

Merzenich MM, Kaas JH, Wall JT, Nelson RJ, Sur M, Felleman DJ. Topographic reorganization of somatosensory cortical areas 3b and 1 in adult monkeys following restricted deafferentation. Neuroscience. 1983a; 8:33–55. [PubMed: 6835522]

Merzenich MM, Kaas JH, Wall JT, Sur M, Nelson RJ, Felleman DJ. Progression of change following median nerve section in the cortical representation of the hand in areas 3b and 1 in adult owl and squirrel monkeys. Neuroscience. 1983b; 10:639–665. [PubMed: 6646426]

Mhatre MC, Pena G, Sieghart W, Ticku MK. Antibodies specific for GABAA receptor alpha subunits reveal that chronic alcohol treatment down-regulates alpha-subunit expression in rat brain regions. J Neurochem. 1993; 61:1620–1625. [PubMed: 8228981]

Mody I. Aspects of the homeostaic plasticity of GABAA receptor-mediated inhibition. J Physiol. 2005; 562:37–46. [PubMed: 15528237]

Mowery TM, Garraghty PE. Nerve-injury induced changes to GluR1 and GluR2/3 sub-unit expression in area 3b of adult squirrel monkeys: Developmental recapitulation? Front Syst Neurosci. 2009; 3:1. [PubMed: 19212458]

Myers WA, Churchill JD, Muja N, Garraghty PE. Role of NMDA receptors in adult primate cortical somatosensory plasticity. J Comp Neurol. 2000; 418:373–382. [PubMed: 10713567]

Navarro X, Vivó M, Valero-Cabré A. Neural plasticity after peripheral nerve injury and regeneration. Prog Neurobiol. 2007; 82:163–201. 2007. [PubMed: 17643733]

Otmakhova NA, Lisman JE. Contribution of Ih and GABAB to Synaptically Induced Afterhyperpolarizations in CA1: A Brake on the NMDA Response. J Neurophysiol. 2004; 92:2027–2039. [PubMed: 15163674]

Pérez-Garci E, Gassmann M, Bettler B, Larkum ME. The GABAB1b isoform mediates long-lasting inhibition of dendritic Ca^{2+} spikes in layer 5 somatosensory pyramidal neurons. Neuron. 2006; 50:603–616. [PubMed: 16701210]

Rakic P, Goldman-Rakic PS, Gallager D. Quantitative autoradiography of major neurotransmitter receptors in the monkey striate and extrastriate cortex. J Neurosci. 1988; 8:3670–3690. [PubMed: 2848104]

Recanzone GH, Merzenich MM, Jenkins WM, Grajski KA, Dinse HR. Topographic reorganization of the hand representation in cortical area 3b owl monkeys trained in a frequency-discrimination task. J Neurophysiol. 1992; 67:1031–1056. [PubMed: 1597696]

Redecker C, Wang W, Fritschy JM, Witte OW, Spary EJ, Maqbool A, Saha S, Batten TF. Widespread and long-lasting alterations in GABA(A)-receptor subtypes after focal cortical infarcts in rats: mediation by NMDA-dependent processes. Science. 1999; 283:74–77. [PubMed: 9872744]

Rivera C, Voipio J, Payne JA, Ruusuvuori E, Lahtinen H, Lamsa K, Pirvola U, Saarma M, Kaila K. The K^+/Clco-transporter KCC2 renders GABA hyperpolarizing during neuronal maturation. Nature. 1999; 397:251–255. [PubMed: 9930699]

Rivera C, Voipio J, Kaila K. Two developmental switches in GABAergic signalling: the K+-Cl- cotransporter KCC2 and carbonic anhydrase CAVII. J Physiol. 2005; 562:27–36. [PubMed: 15528236]

Ronchi G, Nicolino S, Raimondo S, Tos P, Battiston B, Papalia I, Varejão AS, Giacobini-Robecchi MG, Perroteau I, Geuna S. Functional and morphological assessment of a standardized crush injury of the rat median nerve. J Neurosci Methods. 2009; 179:51–7. [PubMed: 19428511]

Rudolph U, Crestani F, Möhler H. GABA(A) receptor subtypes: dissecting their pharmacological functions. Trends Pharmacol Sci. 2001; 22:188–194. [PubMed: 11282419]

Schroeder CE, Seto S, Garraghty PE. Emergence of radial nerve dominance in “median nerve cortex” after median nerve transection in an adult squirrel monkey. J Neurophysiol. 1997; 77:522–526. [PubMed: 9120595]

Sengelaub DR, Muja N, Mills AC, Myers WA, Churchill JD, Garraghty PE. Denervation-induced sprouting of intact peripheral afferents into the cuneate nucleus of adult rats. Brain Res. 1997; 769:256–62. [PubMed: 9374193]

Serafini R, Ma W, Maric D, Maric I, Lahjouji F, Sieghart W, Barker JL. Initially expressed early rat embryonic GABA(A) receptor Cl- ion channels exhibit heterogeneous channel properties. Eur J Neurosci. 1998; 10:1771–1783. [PubMed: 9751149]

Scheperjans F, Grefkes C, Palomero-Gallagher N, Schleicher A, Zilles K. Subdivisions of human parietal area 5 revealed by quantitative receptor autoradiography: a parietal region between motor, somatosensory, and cingulate cortical areas. Neuroimage. 2005; 25:975–992. [PubMed: 15808998]

Shaw C, Cameron L, March D, Cynader M, Zielinski B, Hendrickson A. Pre- and postnatal development of GABA receptors in Macaca monkey visual cortex. J Neurosci. 1991; 11:3943–3959. [PubMed: 1660536]

Silva-Barrat C, Champagnat J, Brailowsky S, Menini C, Naquet R. Relationship between tolerance to GABAA agonist and bursting properties in neocortical neurons during GABA-withdrawal syndrome. Brain Res. 1989; 498:289–298. [PubMed: 2790484]

Standley S, Wagle N, Baudry M. Developmental changes in subcellular AMPA/GluR receptor populations in rat forebrain. Brain Res Dev Brain Res. 1998; 107:277–283.

Steiger JL, Bandyopadhyay S, Farb DH, Russek SJ. cAMP response element-binding protein, activating transcription factor-4, and upstream stimulatory factor differentially control hippocampal GABABR1a and GABABR1b subunit gene expression through alternative promoters. J Neurosci. 2004; 24:115–126.

Sur M, Nelson RJ, Kaas JH. Representations of the body surface in cortical areas 3b and 1 of squirrel monkeys: comparisons with other primates. J Comp Neurol. 1982; 211:177–192. [PubMed: 7174889]

Terunuma M, Vargas KJ, Wilkins ME, Ramírez OA, Jaureguiberry-Bravo M, Pangalos MN, Smart TG, Moss SJ, Couve A. Prolonged activation of NMDA receptors promotes dephosphorylation and alters postendocytic sorting of GABAB receptors. Proc Natl Acad Sci. 2010; 107:13918–23. [PubMed: 20643948]

Thiagarajan TC, Lindskog M, Tsien RW. Adaptation to synaptic inactivity in hippocampal neurons. Neuron. 2005; 47:725–737. [PubMed: 16129401]

Tombari D, Loubinoux I, Pariente J, Gerdelat A, Albucher JF, Tardy J, Cassol E, Chollet F. A longitudinal fMRI study: in recovering and then in clinically stable sub-cortical stroke patients. Neuroimage. 2004; 23:827–839. [PubMed: 15528083]

Turrigiano GG. Homeostatic plasticity in neuronal networks: the more things change, the more they stay the same. Trends Neurosci. 1999; 22:221–227. [PubMed: 10322495]

Vicini S, Ferguson C, Prybylowski K, Kralic J, Morrow AL, Homanics GE. GABA(A) receptor alpha1 subunit deletion prevents developmental changes of inhibitory synaptic currents in cerebellar neurons. J Neurosci. 2001; 21:3009–3016. [PubMed: 11312285]

Vickers JC, Huntley GW, Edwards AM, Moran T, Rogers SW, Heinemann SF, Morrison JH. Quantitative localization of AMPA/kainate and kainate glutamate receptor subunit immunoreactivity in neurochemically identified subpopulations of neurons in the prefrontal cortex of the macaque monkey. J Neurosci. 1993; 13:2982–92. [PubMed: 7687283]

Vigot R, Barbieri S, Bräuner-Osborne H, Turecek R, Shigemoto R, Zhang YP, Luján R, Jacobson LH, Biermann B, Fritschy JM, Vacher CM, Müller M, Sansig G, Guetg N, Cryan JF, Kaupmann K, Gassmann M, Oertner TG, Bettler B. Differential compartmentalization and distinct functions of GABAB receptor variants. Neuron. 2006; 50:589–601. [PubMed: 16701209]

Wall JT, Felleman DJ, Kaas JH. Recovery of normal topography in the somatosensory cortex of monkeys after nerve crush and regeneration. Science. 1983; 221:771–773. [PubMed: 6879175]

Wall JT, Xu J, Wang X. Human brain plasticity: an emerging view of the multiple substrates and mechanisms that cause cortical changes and related sensory dysfunctions after injuries of sensory inputs from the body. Brain Res Rev. 2002; 39:181–215. [PubMed: 12423766]

Wang DD, Kriegstein AR. GABA regulates excitatory synapse formation in the neocortex via NMDA receptor activation. J Neurosci. 2008; 28:5547–5558. [PubMed: 18495889]

Wang X, Tegner J, Constantinidis C, Goldman-Rakic P. Division of labor among distinct subtypes of inhibitory neurons in a cortical microcircuit of working memory. Proc Natl Acad Sci U S A. 2004; 101:1368–1373. [PubMed: 14742867]

Wellman CL, Arnold LL, Garman EE, Garraghty PE. Acute reductions in GABAA receptor binding in layer IV of adult primate somatosensory cortex after peripheral nerve injury. Brain Res. 2002; 954:68–72. [PubMed: 12393234]

White JH, Wise A, Main MJ, Green A, Fraser NJ, Disney GH, Barnes AA, Emson P, Foord SM, Marshall FH. Heterodimerization is required for the formation of a functional GABA(B) receptor. Nature. 1998; 396:679–682. [PubMed: 9872316]

Wieloch T, Nikolich K. Mechanisms of neural plasticity following brain injury. Curr Opin Neurobiol. 2006; 16:258–264. [PubMed: 16713245]

Wigström H, Gustafsson B. Postsynaptic control of hippocampal long-term potentiation. J Physiol (Paris). 1986; 81:228–236. [PubMed: 2883309]

Wilber AA, Southwood CJ, Sokoloff G, Steinmetz JE, Wellman CL. Neonatal maternal separation alters adult eyeblink conditioning and glucocorticoid receptor expression in the interpositus nucleus of the cerebellum. Dev Neurobiol. 2007; 67:1751–1764. [PubMed: 17659594]

Wilber AA, Southwood CJ, Wellman CL. Brief neonatal maternal separation alters extinction of conditioned fear and corticolimbic glucocorticoid and NMDA receptor expression in adult rats. Dev Neurobiol. 2009; 69:73–87. [PubMed: 19025931]

Woldag H, Gerhold LL, de Groot M, Wohlfart K, Wagner A, Hummelsheim H. Early prediction of functional outcome after stroke. Brain Inj. 2006; 20:1047–1052. [PubMed: 17060137]

Xerri C, Stern JM, Merzenich MM. Alterations of the cortical representation of the rat ventrum induced by nursing behavior. J Neurosci. 1994; 14:1710–1721. [PubMed: 8126565]

Young AB, Dauth GW, Hollingsworth Z, Penney JB, Kaatz K, Gilman S. Quisqualateand NMDA-sensitive [3H]glutamate binding in primate brain. J Neurosci Res. 1990; 27:512–521. [PubMed: 1981916]

- Nerve compression injuries induce reorganization prior to reinnervation.
- GluR2/3 containing AMPAR are significantly elevated following reinnervation.
- Inhibitory tone returns following reinnervation.
- Presynaptic GABA autoregulation is significantly elevated in layers VI, V, and VI.
- Postsynaptic NMDAR inhibition is significantly reduced following reinnervation.

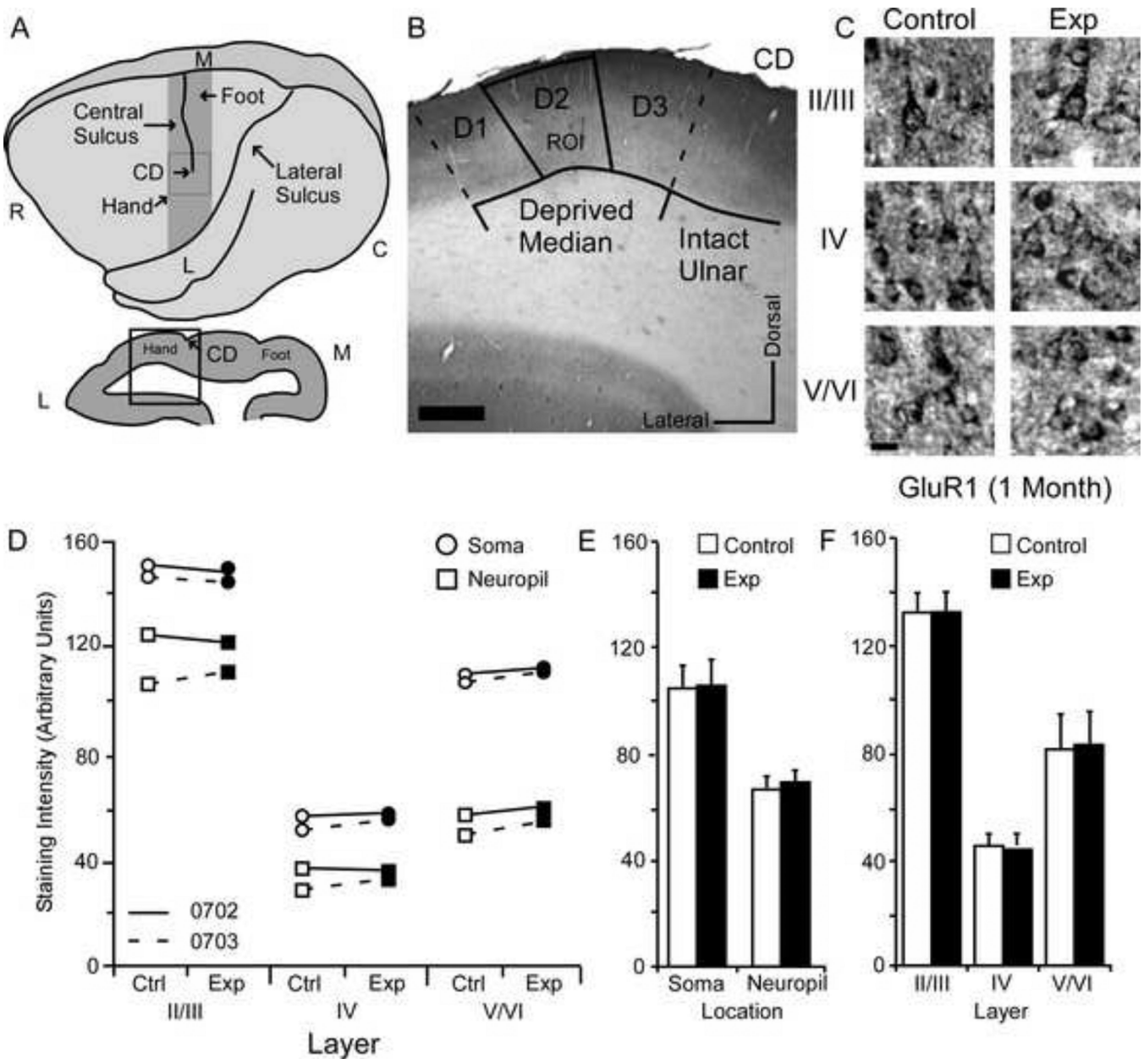

Figure 1.

Changes in **GluR1** receptor subunit staining 1 month after nerve injury. **Figure 1A:** Top: Cartoon of the squirrel monkey cortex identifying area 3b (gray bar), **CD**; *central dimple*, **R**; rostral, **C**; *caudal*, **M**; *medial*, **L**; *lateral*. Bottom: Coronal section through area 3b identifying region of interest (black box), **CD**; *central dimple*, **L**; *lateral*, **M**; *medial*. **Figure 1B:** Photo-micrograph of a control section indicating the sampling region for immunohistochemical quantification of staining intensity (Median Input): scale bar 0.5 mm; **CD** *central dimple*, **ROI** *region of interest*. **Figure 1C:** Photomicrographs showing qualitative examples of **GluR1** soma staining between control and experimental II/III, IV, and V/VI cortical layers 1 month after nerve injury: scale bar 5 μm. **Figure 1D:** Qualitative scatter-plot showing compared **GluR1** staining intensity data for all animals across layer and

location one month after nerve injury. **Figure 1E:** Bar histogram showing the quantified difference in **GluR1** receptor subunit staining between soma and neuropil one month after nerve injury. **Figure 1F:** Bar histogram showing the quantified difference in **GluR1** receptor subunit staining between cortical layers II/III, IV, and V/VI one month after nerve injury.

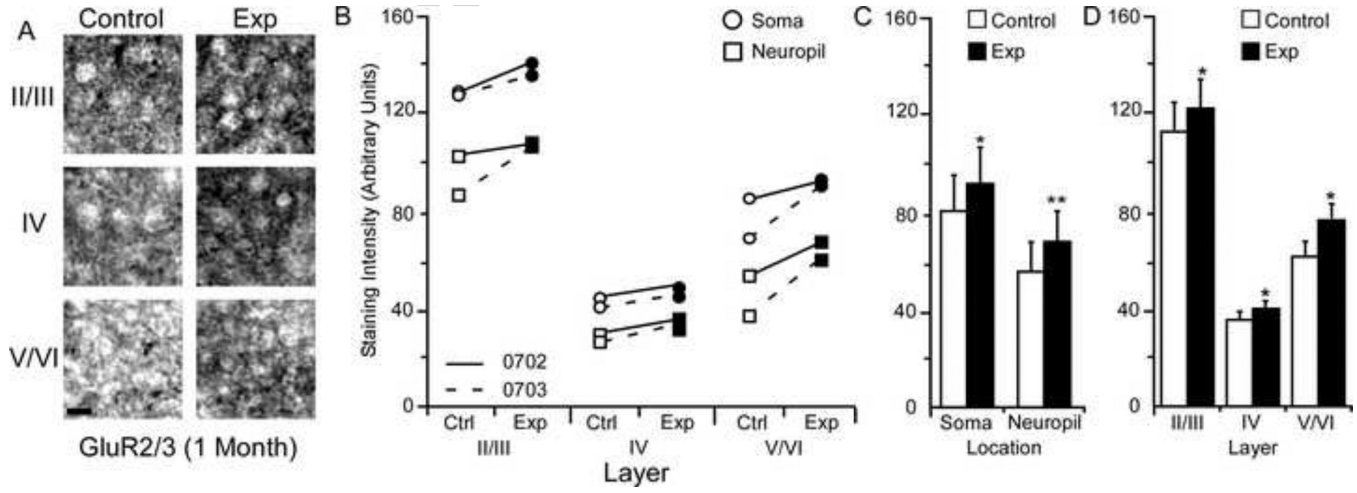

Figure 2.

Changes in **GluR2/3** receptor subunit staining 1 month after nerve injury. **Figure 2A:** Photomicrographs showing qualitative examples of **GluR2/3** soma staining between control and experimental II/III (II/III), IV (VI), and V/VI (V/VI) cortical layers 1 month after nerve injury: scale bar 5 μm. **Figure 2B:** Qualitative scatter-plot showing compared **GluR2/3** staining intensity data for all animals across layer and location one month after nerve injury. **Figure 2C:** Bar histogram showing the quantified difference in **GluR2/3** receptor subunit staining between soma and neuropil one month after nerve injury. **Figure 2D:** Bar histogram showing the quantified difference in **GluR2/3** receptor subunit staining between cortical layers II/III, IV, and V/VI one month after nerve injury. * = $p < .05$; ** = $p < .01$; *** = $p < .001$.

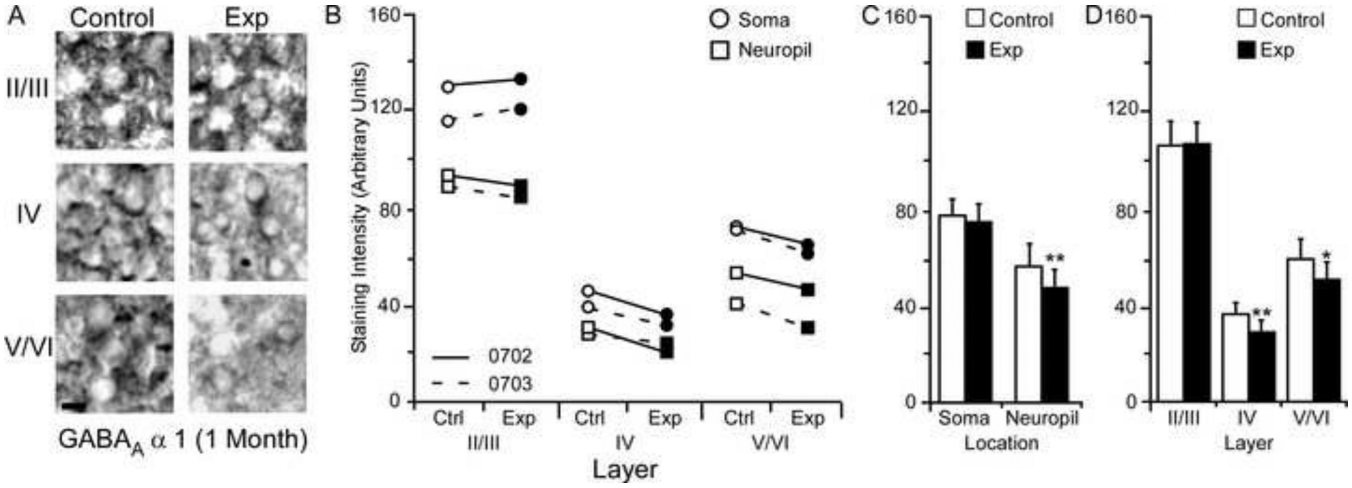

Figure 3.

Changes in **GABA$_A$ α1** receptor subunit staining 1 month after nerve injury. **Figure 3A:** Photomicrographs showing qualitative examples of **GABA$_A$ α1** somal staining between control and experimental cortical layers II/III, IV, and V/VI 1 month after nerve injury: scale bar 5 μm. **Figure 3B:** Qualitative scatter-plot showing compared **GABA$_A$ α1** staining intensity data for all animals across layer and location one month after nerve injury. **Figure 3C:** Bar histogram showing the quantified difference in **GABA$_A$ α1** receptor subunit staining between soma and neuropil one month after nerve injury. **Figure 3D:** Bar histogram showing the quantified difference in **GABA$_A$ α1** receptor subunit staining between cortical layers II/III, IV, and V/VI one month after nerve injury. * = p < .05; ** = p < .01; *** = p <. 001.

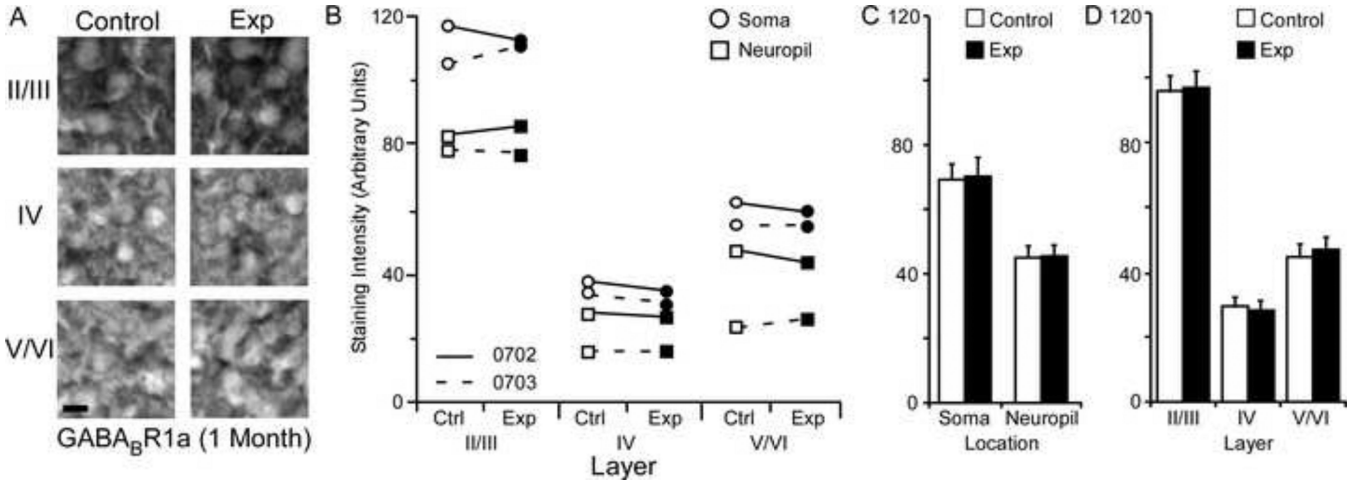

Figure 4.

Changes in **GABA$_B$R1a** receptor subunit staining 1 month after nerve injury. **Figure 4A:** Photomicrographs showing qualitative examples of **GABA$_B$R1a** soma staining between control and experimental cortical layers II/III , IV, and V/VI 1 month after nerve injury: scale bar 5 μm. **Figure 4B:** Qualitative scatter-plot showing compared **GABA$_B$R1a** staining intensity data for all animals across layer and location one month after nerve injury. **Figure 4C:** Bar histogram showing the quantified difference in **GABA$_B$R1a** receptor subunit staining between soma and neuropil one month after nerve injury. **Figure 4D:** Bar histogram showing the quantified difference in **GABA$_B$R1a** receptor subunit staining between cortical layers II/III, IV, and V/VI one month after nerve injury. * = p < .05; ** = p < .01; *** = p <. 001.

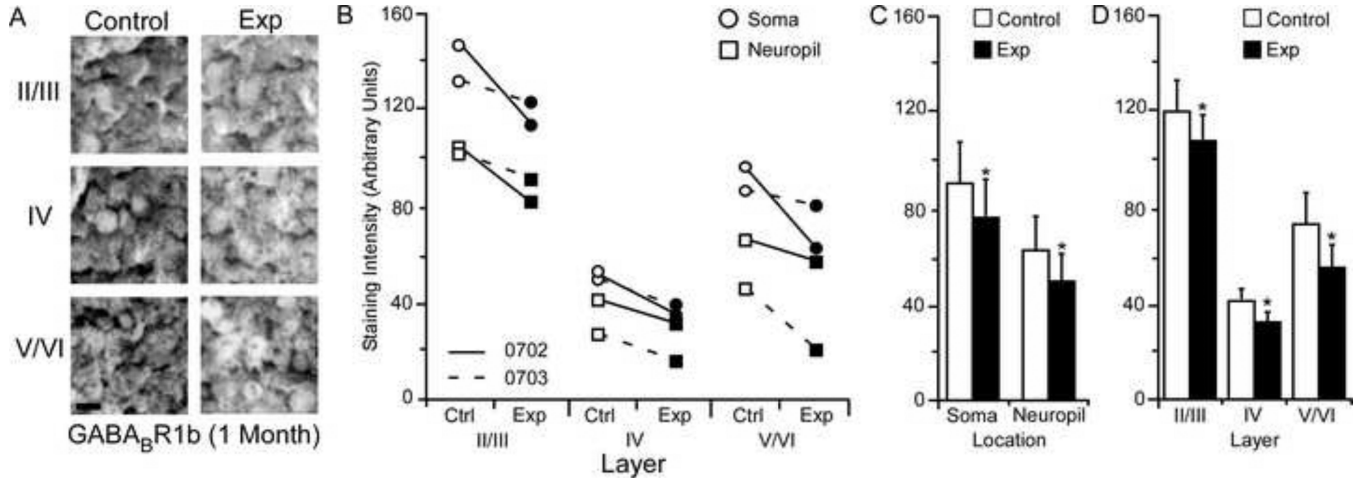

Figure 5.

Changes in **GABA$_B$R1b** receptor subunit staining 1 month after nerve injury. **Figure 5A:** Photomicrographs showing qualitative examples of **GABA$_B$R1b** soma staining between control and experimental cortical layers II/III, IV, and V/VI, 1 month after nerve injury: scale bar 5 μm. **Figure 5B:** Qualitative scatter-plot showing compared **GABA$_B$R1b** staining intensity data for all animals across layer and location one month after nerve injury. **Figure 5C:** Bar histogram showing the quantified difference in **GABA$_B$R1b** receptor subunit staining between soma and neuropil one month after nerve injury. **Figure 5D:** Bar histogram showing the quantified difference in **GABA$_B$R1b** receptor subunit staining between cortical layers II/III, IV, and V/VI one month after nerve injury. * = $p < .05$; ** = $p < .01$

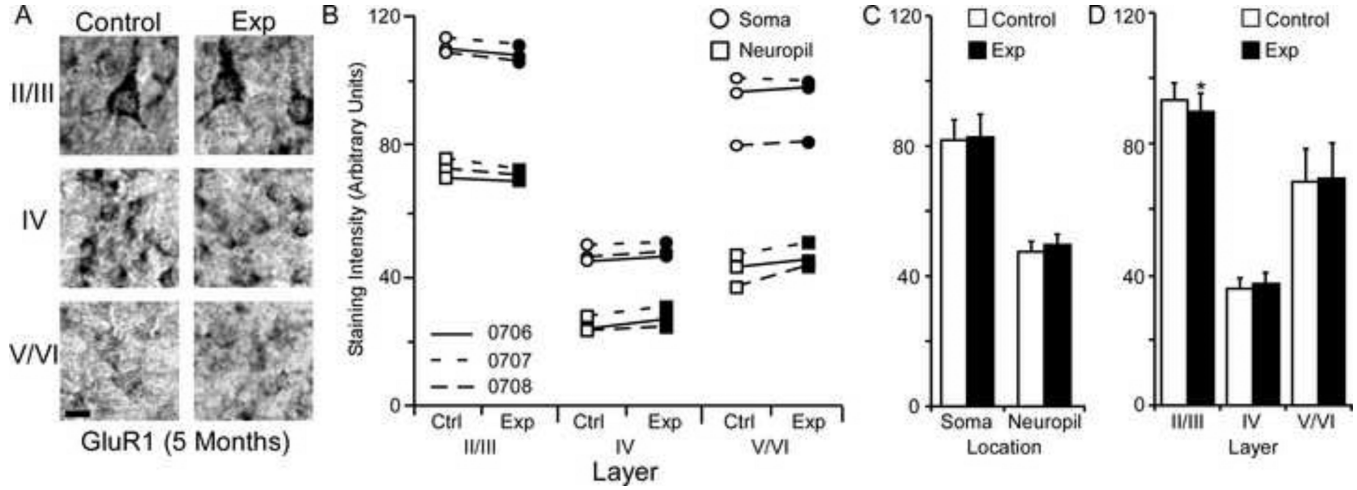

Figure 6.

Changes in **GluR1** receptor subunit staining 5 months after nerve injury. **Figure 6A:** Photomicrographs showing qualitative examples of **GluR1** soma staining between control and experimental II/III, IV, and V/VI cortical layers five months after nerve injury: scale bar 5 μm. **Figure 6B:** Qualitative scatter-plot showing compared **GluR1** staining intensity data for all animals across layer and location five months after nerve injury. **Figure 6C:** Bar histogram showing the quantified difference in **GluR1** receptor subunit staining between soma and neuropil five months after nerve injury. **Figure 6D:** Bar histogram showing the quantified difference in **GluR1** receptor subunit staining between cortical layers II/III, IV, and V/VI five months after nerve injury. * = $p < .05$

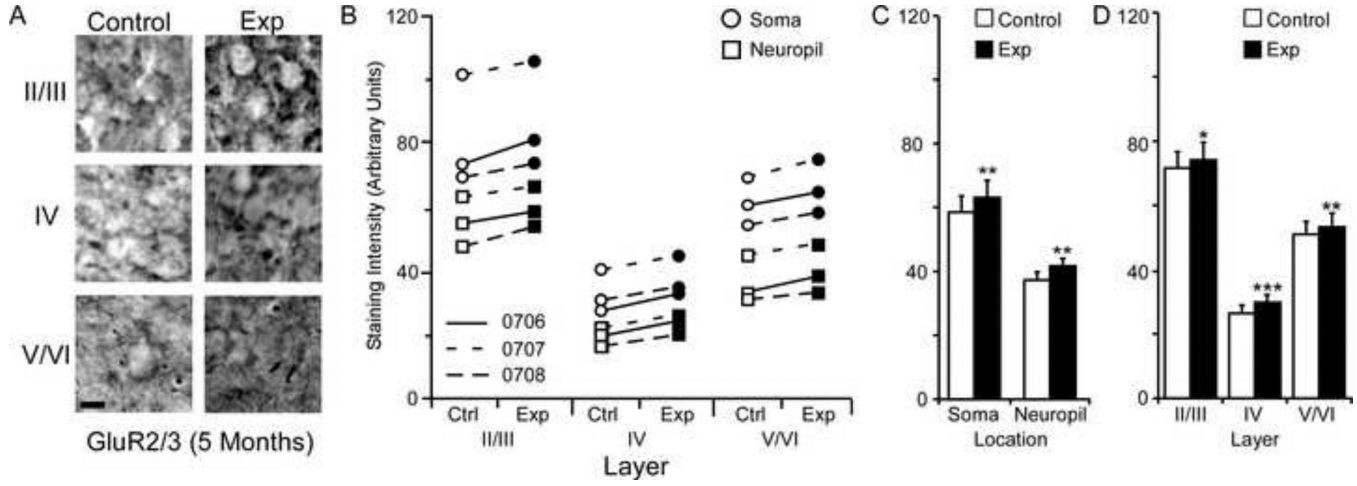

Figure 7.

Changes in **GluR2/3** receptor subunit staining 5 months after nerve injury. **Figure 7A:** Photomicrographs showing qualitative examples of **GluR2/3** soma staining between control and experimental II/III, IV, and V/VI cortical layers five months after nerve injury: scale bar 5 μm. **Figure 7B:** Qualitative scatter-plot showing compared **GluR2/3** staining intensity data for all animals across layer and location five months after nerve injury. **Figure 7C:** Bar histogram showing the quantified difference in **GluR2/3** receptor subunit staining between soma and neuropil five months after nerve injury. **Figure 7D:** Bar histogram showing the quantified difference in **GluR2/3** receptor subunit staining between cortical layers II/III, IV, and V/VI five months after nerve injury. * = $p < .05$; ** = $p < .01$; *** = $p < .001$.

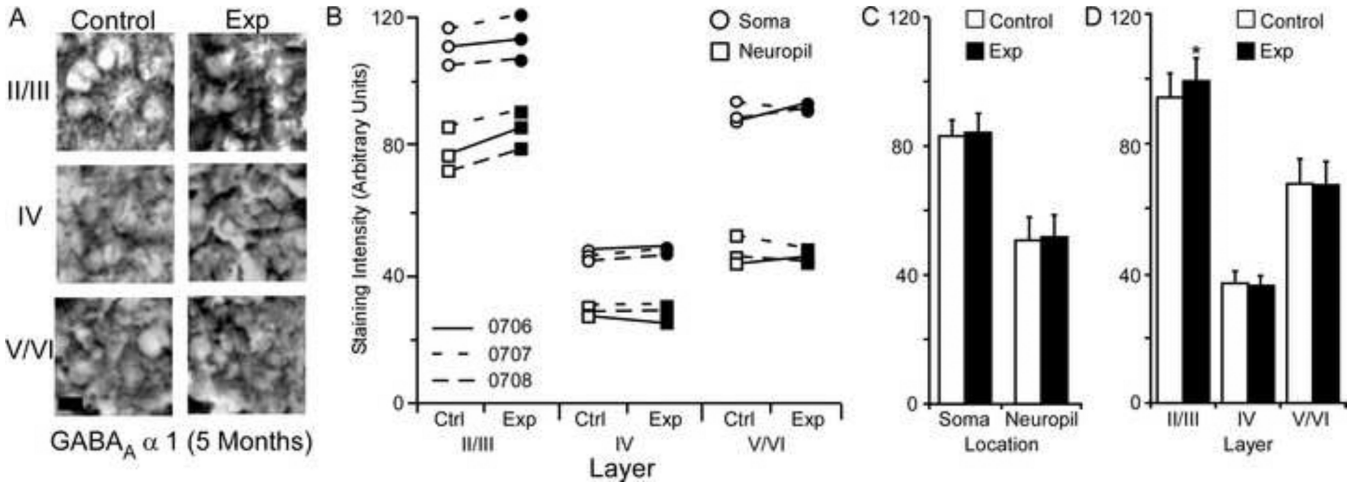

Figure 8.

Changes in **GABA$_A$ α1** receptor subunit staining 5 months after nerve injury. **Figure 8A:** Photomicrographs showing qualitative examples of **GABA$_A$ α1** soma staining between control and experimental II/III, IV, and V/VI cortical layers five months after nerve injury: scale bar 5 μm. **Figure 8B:** Qualitative scatter-plot showing compared **GABA$_A$ α1** staining intensity data for all animals across layer and location five months after nerve injury. **Figure 8C:** Bar histogram showing the quantified difference in **GABA$_A$ α1** receptor subunit staining between soma and neuropil five months after nerve injury. **Figure 8D:** Bar histogram showing the quantified difference in **GABA$_A$ α1** receptor subunit staining between cortical layers II/III, IV, and V/VI five months after nerve injury. * = $p < .05$

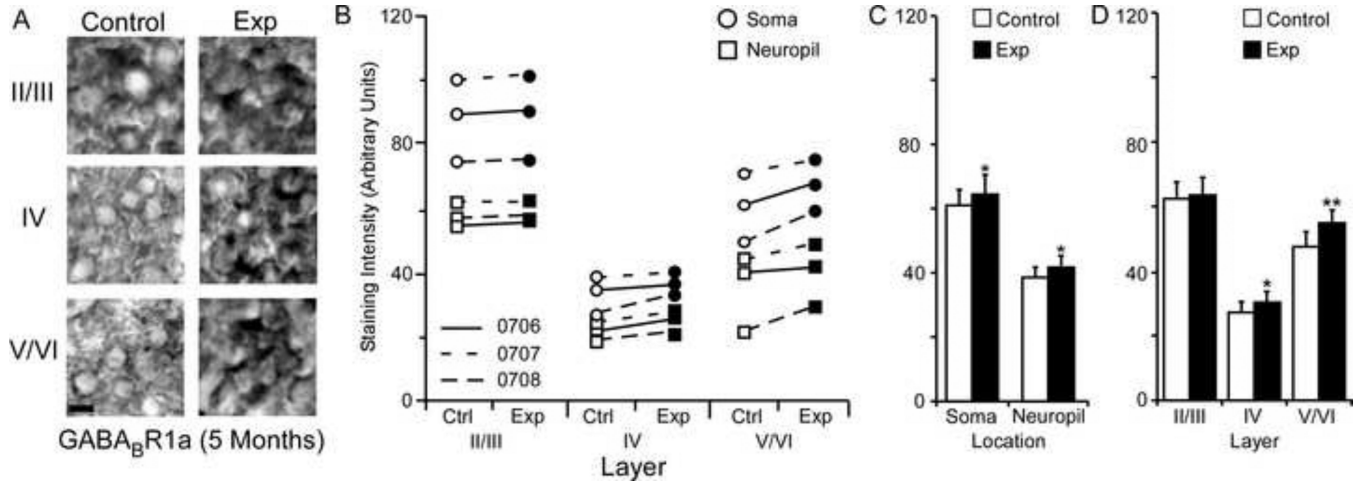

Figure 9.

Changes in **GABA$_B$R1a** receptor subunit staining 5 months after nerve injury. **Figure 9A:** Photomicrographs showing qualitative examples of **GABA$_B$R1a** soma staining between control and experimental II/III, IV, and V/VI cortical layers five months after nerve injury: scale bar 5 μm. **Figure 9B:** Qualitative scatter-plot showing compared **GABA$_B$R1a** staining intensity data for all animals across layer and location five months after nerve injury. **Figure 9C:** Bar histogram showing the quantified difference in **GABA$_B$R1a** receptor subunit staining between soma and neuropil five months after nerve injury. **Figure 9D:** Bar histogram showing the quantified difference in **GABA$_B$R1a** receptor subunit staining between cortical layers II/III, IV, and V/VI five months after nerve injury. * = $p < .05$; ** = $p < .01$

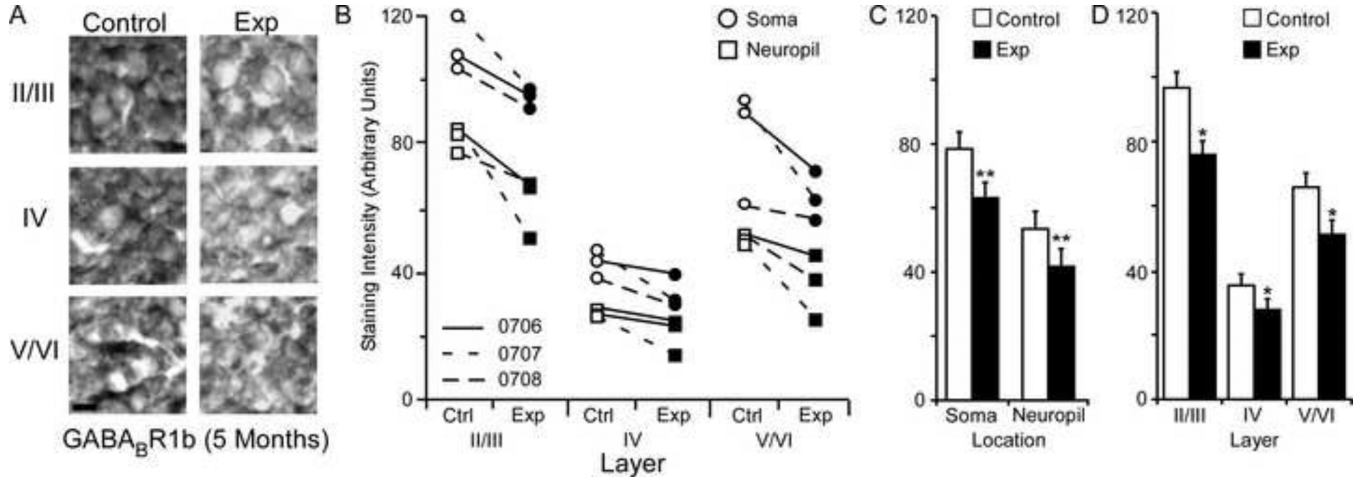

Figure 10.

Changes in **GABA$_B$R1b** receptor subunit staining 5 months after nerve injury. **Figure 10A:** Photomicrographs showing qualitative examples of **GABA$_B$R1b** soma staining between control and experimental II/III, IV, and V/VI cortical layers five months after nerve injury: scale bar 5 μm. **Figure 10B:** Qualitative scatter-plot showing compared **GABA$_B$R1b** staining intensity data for all animals across layer and location five months after nerve injury. **Figure 10C:** Bar histogram showing the quantified difference in **GABA$_B$R1b** receptor subunit staining between soma and neuropil five months after nerve injury. **Figure 10D:** Bar histogram showing the quantified difference in **GABA$_B$R1b** receptor subunit staining between cortical layers II/III, IV, and V/VI five months after nerve injury. * = $p < .05$; ** = $p < .01$

Table 1

List of antibodies used in this study. Antibodies are listed by name, subunit specific target, manufacturer, and dilution used in this study.

Antibody	Immunogen	Manufacturer	Dilution
GluR1	106 kDa (monomer) and 200 kDa (dimer) of rat GluR1 receptor	Chemicon (Billerica), Rabbit monoclonal, # 05-855R	1:1000
GluR2/3	Peptide corresponding to amino acid residues from the C-terminus of rat GluR2/3 receptor	Thermo Scientific (Rockford), Rabbit polyclonal # PA1 -4660	1:1000
$GABA_A\alpha 1$	51 kDa C-Terminus of rat $GABA_A\alpha$ 1 subunit	Thermo Scientific (Rockford), Rabbit polyclonal, # PA1-4658	1:1000
$GABA_B$1a	18aa peptide from N-Terminus of rat $GABA_B$1a subunit	Alpha Diagnostic (San Antonio), Rabbit polyclonal, #GBR1A11-A	1:1000
G ABA_B 1b	16aa peptide from N-Terminus of rat $GABA_B$1b subunit	Alpha Diagnostic (San Antonio), Rabbit polyclonal, #GBR1B11-A	1:1000